

# Simulated prosthetic visual fixation, saccade, and smooth pursuit

Luke E. Hallum<sup>a,c</sup>, Gregg J. Suaning<sup>a,b</sup>, David S. Taubman<sup>c</sup>, Nigel H. Lovell<sup>a,d,\*</sup>

<sup>a</sup> Graduate School of Biomedical Engineering, University of New South Wales, Sydney 2052, Australia

<sup>b</sup> School of Engineering, University of Newcastle, Newcastle, Australia

<sup>c</sup> School of Electrical Engineering and Telecommunications, University of New South Wales, Sydney, Australia

<sup>d</sup> National ICT Australia (NICTA), Australia

Received 19 January 2004; received in revised form 21 July 2004

## Abstract

A visual tracking task was administered to 20 subjects afforded simulated prosthetic vision (a phosphene array); a total of 3 h data was taken from each subject over the course of 10 visits. The experiment assessed prosthetic visual fixation, saccade and smooth pursuit and the effect of practice. Further, we demonstrated an image analysis technique that assisted fixation and pursuit (but not saccade) accuracy, and required less vigorous movement of the phosphene array in pursuing the target. As measured by mean deviation from the target, fixation and pursuit accuracies were improved by 8.3 and 3.3 min of visual arc, respectively (35.8% and 6.8%), for inter-phosphene spacing of 1.9°. The analysis technique, involving overlapping Gaussian kernels, was an heuristic design; this is the first step of an iterative, experimental approach to devising effective image analysis to be contained in an electronic vision prosthesis. The approach should ultimately afford implanted patients improved prosthetic visual function.

© 2004 Elsevier Ltd. All rights reserved.

**Keywords:** Prosthetic vision; Vision prosthesis; Psychophysics; Linear filtering; Visual tracking

## 1. Introduction

For sufferers of outer retinal degeneration (e.g., age-related macular degeneration and retinitis pigmentosa), stimulating electrodes at the vitreoretinal interface are shown to elicit discrete percepts—so-called “phosphenes”—in the visual field (Humayun et al., 1996; Humayun et al., 1999). This psychophysical result is consistent with in vivo and in vitro animal studies (Eysel et al., 2002; Humayun, Propst, de Juan, McCormick, & Hickingbotham, 1994), and is attributed to the high survival rates, relative to the outer retina, of inner retinal layers (Stone, Barlow, Humayun, de Juan, & Milam, 1992). The elicitation of phosphenes is the cornerstone of ongoing attempts by the authors’ group and others (for re-

view, see Zrenner, 2002) to provide an electronic retinal prosthesis. Here, electrodes, together comprising an intraocularly implantable array, are independently actuated by an implanted neurostimulation integrated circuit (IC); central to the authors’ application-specific IC (Suaning & Lovell, 2001), and others (Hornig & Eckmiller, 2002; Liu et al., 2000), is the ability to modulate stimulation profiles at electrodes independently, and thus modulate phosphenes. The approach bears resemblance to that of the cochlear implant, where the function of degenerate hair cells of the inner ear is replaced by an implanted array of electrodes stimulating spiral ganglion cells (Rubinstein & Miller, 1999).

Phosphene representations of visual stimuli have been simulated in previous work, central to which is that of Cha and colleagues (Cha, Horch, & Normann, 1992a, 1992b; Cha, Horch, Normann, & Boman, 1992). Those authors devised a so-called “pixelized vision simulator”: a portable television set worn on the head and viewed

\* Corresponding author. Tel.: +61 2 9385 3922; fax: +61 2 9663 2108.

E-mail address: [n.lovell@unsw.edu.au](mailto:n.lovell@unsw.edu.au) (N.H. Lovell).

through a mask of pinholes. That is, the “underlying” stimulus was spatially impulsively sampled. This set-up was used to assess the effect of phosphene density, and the extent of the visual field occupied by phosphene arrays, on subjects’ mobility. The walking speed and collision rate of subjects in an indoor maze of obstacles was examined; it was demonstrated that a 25-by-25 array of phosphenes occupying the central 30° of the visual field (corresponding to an inter-phosphene spacing of 1.2°) allowed walking speed comparable to that of a control subject. Further, subjects were administered tumbling-E trials to assess acuity (Cha, Horch, & Normann, 1992b). When inter-phosphenes spacing was 3.2 min of visual arc, regardless of whether 100- or 1024-phosphene arrays were used, subjects were afforded 20/26 Snellen acuity.

Subsequent work to that of Cha has been very much in the same spirit: that “three parameters are important in determining the quality of a pixelized image: the number of pixels, their density, and their range of intensities” (Cha et al., 1992b). Humayun (2001) used a head-mounted display and set phosphene array geometries that better approximate the state of the art of implantable retinal prosthetics. He assessed Snellen acuity, recognition of simple objects (such as spoons, plates, pens, and cups), and subjects’ abilities to wield simple household objects. Four-by-four, 6-by-10, and 16-by-16 phosphene arrays were used occupying up to 36-by-48° of the central visual field. To Humayun’s method, Thompson and colleagues (Thompson, Barnett, Humayun, & Dagnelie, 2003) added the parameters phosphene size, inter-phosphene spacing, and phosphene drop-out; four subjects were required to recognize faces. Hayes and colleagues (Hayes et al., 2003) examined Snellen acuity, hand–eye coordination, and the recognition of simple objects. Humayun (2001), Thompson et al. (2003), and Hayes et al. (2003) used simple regional averaging of the “underlying” stimulus to drive their phosphene arrays, referred to as “box” filtering (Thompson et al., 2003), or the “mean luminance” beneath the aperture of a phosphene (Hayes et al., 2003).

### 1.1. Rationale of the study

The primary goal of the present work is to address the image analysis to be contained in a retinal prosthesis. Our approach uses an analysis–synthesis framework, separating the processing of visual stimuli (analysis) from their representation via phosphenes (synthesis). For the present study, we have set synthesis parameters (including the sizes of phosphenes, their separation, their modulation, and the overall geometry of the phosphene array) in correspondence with existing implantable electrode array designs (Suaning, Lovell, & Kwok, 2003).

The existing psychophysics work, discussed in Section 1, ignores image analysis beyond trivial implemen-

tations; its focus is the quantification of the usefulness of prosthetic vision (mobility, reading speed, face recognition). The present work assesses an analysis scheme designed intuitively so as to encode extra information in the phosphene image. We contrast the effect of this scheme with those of existing, trivial implementations. We do not imagine the scheme to be optimal, but rather seek to show an effect above and beyond existing implementations. This would justify future work towards its optimization, central to which would be data gathered from the present experiment. That is, this work may be thought of as the first step of an iterative, experimental process of designing image analysis for a retinal prosthesis.

It is useful to draw parallels between the present work and work on auditory neuroprostheses. With a mind to devising effective speech processing techniques, it is common practice by “cochlear” groups to simulate degraded auditory signals—“low-channel” signals with information content similar to those perceived by auditory neuroprosthesis implantees—on loudspeakers played to the normally hearing (Arbogast, Mason, & Kidd, 2002; Dorman, Loizou, & Fitzke, 1998; Throckmorton & Collins, 2002). The overall improvement in recent decades of monosyllabic word recognition in cochlear implantees (10% in the 1980s versus approximately 45% in 1999) is one-third attributed to improved speech processing (Rubinstein & Miller, 1999). With regard to retinal prosthetics, clinical trials of an epiretinal device have recently begun in the United States (Humayun et al., 2003a, 2001); the retinal prosthesis is in its infancy and it is not surprising that there are currently few data concerning the integration of image processing techniques and retinal neuroprostheses. An important difference between auditory and visual simulations, however, is that the role of auditory subjects is passive (their ears being immobile), whereas the role of visual subjects is active (they are required to scan the visual stimuli).

The following explains the rationale of the present experimental set-up. A moving target serves as the stimulus; it is represented on a phosphene array that the subject may move around the computer monitor (using a joystick), “over” the stimulus. In turn, the subject’s eyes survey the phosphene array. That is, phosphene array movement and the subject’s gaze are uncoupled. It is important to note, however, that by surveying the phosphene array the subject gains no information, assuming that the relatively large changes in phosphene sizes are detected by the relative abundance of photoreceptors in the peripheral macula. The primary goal of the present study is to quantify the effect of the extra information, coded via the intuitive scheme, when presented within the confines (stimulus parameters) of prosthetic vision. That is, can subjects use this extra information to better localize the target? Is learning required to do so? And if so, how much?

Why use a small target as stimulus? Early generations of retinal prostheses will feature low-density implantable electrode arrays. This low density is due, first, to the electrotonicity of the retina being such that phosphenes will interact if electrodes, as per current designs, are too close together. Second, very small electrodes, being more resistive, pose power constraints on an implantable, microelectronic neurostimulator, and may make for charge densities in tissue that exceed safe limits. Where a low density of electrodes (and therefore phosphenes) prevails, hyperacuity, or the ability to discern details smaller than inter-electrode (inter-phosphene) separation, is central.

Of secondary interest in the present study is subjects' movement of the phosphene array. Central to the effective use of any phosphene array is its movement; it is therefore important to quantify and contrast the movement pertaining to different image analysis schemes. We take up this point, in light of our results, in Section 4.

## 2. Methods

### 2.0.1. Participants

Twenty naïve subjects (16 males; 4 females) with normal, or corrected-to-normal, vision volunteered for the study. Each subject visited the laboratory 10 times over the course of one month, with no two visits occurring on the same day. Each visit comprised approximately 20 min tracking—two 10 min blocks separated by a rest of several minutes. Each block comprised 33 tracking tasks (tests), each of approximately 15 s duration.

### 2.0.2. Set-up

Simulated prosthetic vision was rendered on a computer monitor viewed binocularly from 70 cm by the subject, a distance stabilized by way of a chinrest. The manipulandum was a potentiometer joystick connected to the serial port of the computer. Software was developed by the authors based chiefly on OpenGL, a cross-platform standard for rendering and hardware acceleration (<http://www.opengl.org>).

### 2.0.3. Functional set-up

Fig. 1 depicts the functional set-up. For each test, the stimulus—a moving target—was represented to the subject by way of a phosphene array; the subject was required to track the target with the central phosphene of the array. To do so, the phosphene array could be moved around the monitor by manipulation of the joystick. The phosphene array comprised 23 phosphenes arranged in a regular, hexagonal mosaic. The phosphene array may be thought of as a synthesis stage with several

parameters: number of phosphenes (23); the hexagonal arrangement of phosphenes; the inter-phosphene separation (114.5 min of visual arc); phosphene size when maximally actuated (87.3 min of visual arc). An analysis stage comprising 23 spatial filters was functionally attached to the synthesis stage. It is convenient to think of the analysis stage as unseen, and underlying the synthesis stage (that is, both stages could be moved around the monitor). The locations of spatial filters corresponded to the locations of phosphenes; the operation of any one spatial filter on the underlying stimulus modulated the corresponding phosphene. The sizes of phosphenes were modulated according to this operation; phosphenes were uniformly white.

### 2.0.4. Analysis stages (Schemes)

The experiment assessed the efficacy of three different analysis stages, or filtering schemes: Q0, Q1, and Q2, as depicted in Fig. 1. Scheme Q0 impulsively sampled the stimulus at the 23 locations, in a similar approach to that of Cha et al. (1992a, 1992b); (Cha, Horch, Normann et al., 1992): each phosphene was modulated according to the intensity of the directly underlying stimulus pixel. As per Section 4, phosphene sizes were modulated. Therefore, since stimuli involved high-intensity targets (white on black), for Q0, any given phosphene was therefore either unactivated, or maximally activated (subtending 87.3 min of visual arc). Scheme Q1 regionally averaged the underlying stimulus, in a similar approach to that of Humayun (2001), Hayes et al. (2003), and Thompson et al. (2003); the total region underlying the phosphene array was, in effect, tiled by hexagonal spatial filters. Thus, phosphenes were modulated according to the average intensity of the underlying region. Scheme Q2 involved Gaussian spatial filters with standard deviation 34.4 min of visual arc. By way of control, the stimulus was presented through a “clear” window, the same size as the phosphene array, with a red circle indicating the window's centre.

### 2.0.5. Stimuli

All tests involved a small, white target (35.8-by-35.8 arcmin) which moved on a black background. The target ranged within a circular area of diameter approximately 16.7 arcdeg, and described a randomly generated S-shaped motion (see Fig. 1). The stimuli were derived from those originally used by Rashbass (1961) (see also Leigh & Zee, 1999); we substituted the S-shaped target motion for what is usually a linear ramp. The presentation of stimuli were randomized such that each was presented only once with each filtering scheme over the course of a visit, and no stimulus was tested twice running.

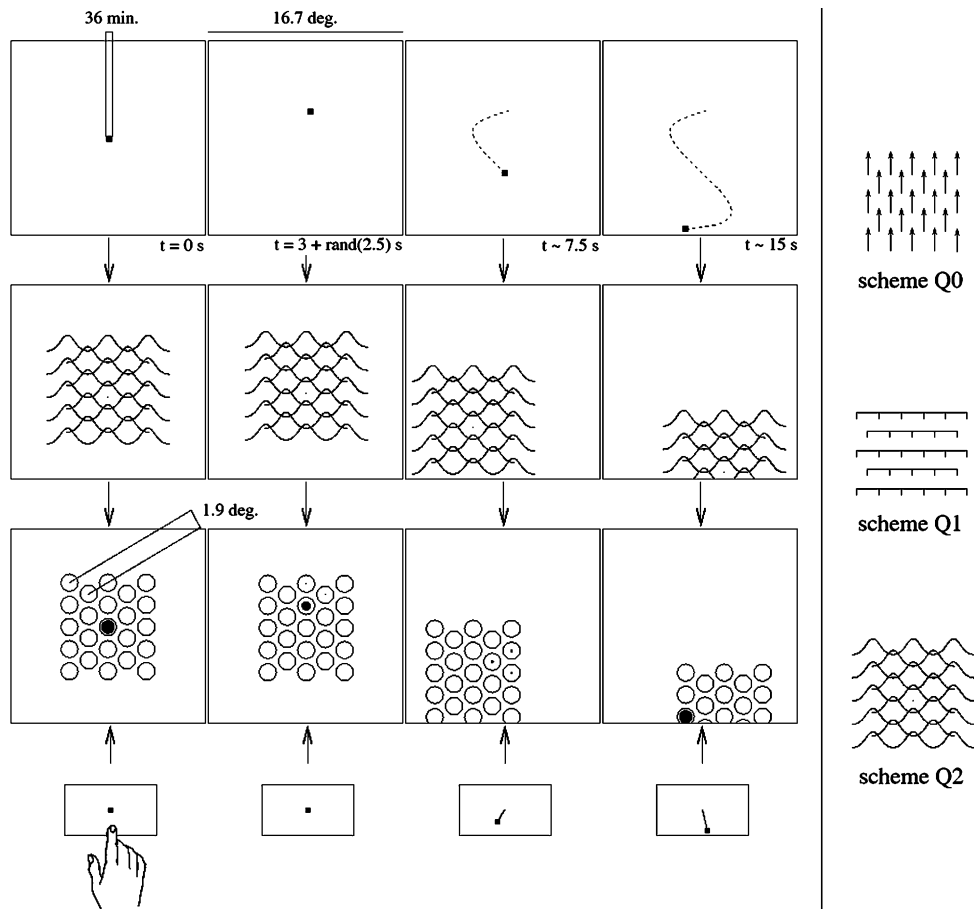


Fig. 1. The functional set-up of the experiment. A typical stimulus motion is depicted in the top row: the target initially appears at a randomly generated point within 15 arcmin of the centre of the monitor (top row, column 1); after some random period between 3.0 and 5.5 s, the target is stepped through 150 arcmin in a random direction to the “step point” (column 2); the target then follows a smooth, S-shaped course (column 3), to a “peripheral point” (column 4), colinear with the step point and the centre of the screen. The local maximum and minimum of the *S* are randomly generated and spline interpolated. Throughout the experiment, the average target speed was 1.7 arcdeg/s (s.d. = 0.7). At each point in time the stimulus is analyzed by the scheme in question (second row); the outcome of this analysis activates phosphenes in the synthesis—the array of phosphenes viewed by the subject (third row). Note that sizes of phosphenes are activated. The subject moves the phosphene array around the monitor by manipulating a joystick (fourth row). The scheme may be conceptualized as being “attached” to the phosphene array, and the stimulus as “underlying” the phosphene array and scheme. Note that black and white have been inverted in rows 1 and 3 for the sake of picture clarity. On the right, the three image analysis schemes in question are depicted: impulsive sampling (scheme Q0), regional averaging (Q1), and Gaussian filtering (Q2) (see Section 2.0.4 in the text). The experiment compares the effect of each scheme on tracking the target, which involves prosthetic visual fixation, saccade, and pursuit.

## 2.0.6. Measures

For each test, we generated two time series,  $f_{sfvt}$  and  $p_{sfvt}$  (fixation and pursuit<sup>1</sup>; sth subject, fth filtering scheme, vth visit, tth test). Each signal is the deviation of the joystick position,  $j_{sfvt}$ , from the target position,  $t_{sfvt}$ ;  $f_{sfvt}$  pertains to deviation while the target is stationary (that is, fixation);  $p_{sfvt}$  to deviation from the moving

target (that is, pursuit). The joystick position corresponds to the position of the central phosphene of the array, or of the red circle for control. Joystick position was sampled at approximately 50 Hz. At the conclusion of the experiment, all signals were low-pass filtered at 25 Hz cut-off using Matlab (1999, version 5.3) forming series  $f_{sfvt}$  and  $p_{sfvt}$  of equal length. The statistics,  $\overline{f_{sfvt}}$  and  $\overline{p_{sfvt}}$ , were then calculated—the mean deviation, for fixation and pursuit, respectively, from the target for a given subject, visit, and filtering scheme, collapsed across tests. These statistics were used for measurement of fixation and pursuit accuracy, respectively.

For measuring saccade latency and end-point deviation, we examined the derivative of joystick position,

<sup>1</sup> Throughout the manuscript, we use the terms “fixation”, “saccade”, and “pursuit”. The reader should note that these are in fact manual analogues of oculomotor behavior. Strictly speaking, as per the manuscript title, the terms “prosthetic visual fixation”, “prosthetic visual saccade”, and “prosthetic visual pursuit” are more accurate.

$j_{sft}^i$ . Once the target is in motion, an initial period of spatial stasis of  $j_{sft}$  (the velocity criterion used was  $<1.2\text{deg/s}$ ) corresponds to the pre-planning phase of the saccade. The duration of this stasis is taken as the latency. Latency is followed by an acceleration and deceleration of  $j_{sft}$ , prior to a second period of spatial stasis. The deviation from the target on reaching this second period of spatial stasis was taken as the end-point deviation.

We define target loss as the instance of the target straying outside the boundary of the phosphene array, or outside the clear window in the control case, and thus becoming “invisible”. As a means of assessing subjects’ learning, for pursuit, we measured target loss at visit 1 and visit 10 for each scheme. This discrepancy was then  $t$ -tested (paired, two-tailed).

We calculated the root-mean-square (RMS) velocities and accelerations for each pursuit deviation signal at visit 10,  $p_{sf10t}$ , and then collapsed this data across tests. This allowed the comparison of the differential effect of schemes on velocity and acceleration after practice. To do so, we first computed the Fourier spectrum,  $\mathcal{F}_{sf10t}$ , for each pursuit deviation,  $p_{sf10t}$ . For each subject, an average spectrum for each scheme was then obtained by collapsing across tests,  $\mathcal{F}_{sf10}$ . (average spectra for schemes, as depicted in Fig. 7, were obtained by further collapsing across subjects,  $\mathcal{F}_{.f10}$ ). Since time-domain differentiation is equivalent filtering by  $-j\omega$  in the Fourier domain, we applied  $-j\omega$  and  $-\omega^2$  to the Fourier spectra  $\mathcal{F}_{sf10}$ . We then integrated the power spectra over the 99.9%-bandwidth, and employed Parseval’s generalized relation

$$\int_{-\infty}^{\infty} [f(t)]^2 dt = 1/2\pi \int_{-\infty}^{\infty} |\hat{f}(\omega)|^2 d\omega, \quad (1)$$

to obtain the RMS velocities and accelerations of  $p_{sf10}$ . Fourier spectra were calculated via FFTW (Frigo & Johnson, 1998), an implementation of the Fast Fourier Transform.

## 2.1. Statistical methods

In assessing the differential effect of schemes (typically that of Q1 and Q2) on fixation, saccade latency and end-point deviation, and pursuit, we repeatedly employed a three-way ANOVA in *subject*, *scheme*, and *visit*, with correction for repeated measures, on data pooled across two schemes. In assessing the *visit* effect, and the effect of *subject*, for individual schemes, the same ANOVA was employed on unpooled data. In assessing target loss during pursuit for visits 1 and 10, a paired, two-tailed Student’s  $t$ -test was employed. In assessing sensor array movement for visit 10, namely the differential effect of schemes Q1 and Q2 on sensor array velocities and accelerations, we employed paired, two-tailed  $t$ -tests on the RMS velocities and accelerations, by subject, inherent to each scheme. Stata (2000) was used for all statistical calculations.

## 3. Results

### 3.1. Fixation, saccade, pursuit accuracy

Fig. 2 depicts three raw traces; pursuit for schemes Q1 and Q2 was more accurate than that of Q0, for which subjects learned to move the phosphene array in a more rapid, nystagmus-like fashion. Fig. 3(a) demonstrates the learning effect for fixation for all schemes and for control. With practice, subjects were able to fixate the target with better accuracy. The bulk of learning, for all schemes and for control, had taken place at the conclusion of visit four—that is, after approximately 16min fixation practice. The efficacy of scheme Q2 relative to Q1 developed with practice: at the conclusion of visit one, subjects fixated with comparable accuracy (deviation Q1: 33.2arcmin; deviation Q2: 31.9arcmin); by the conclusion of visit four, subjects were better able to fixate the target by 8.9arcmin (Q1: 24.8arcmin; Q2:

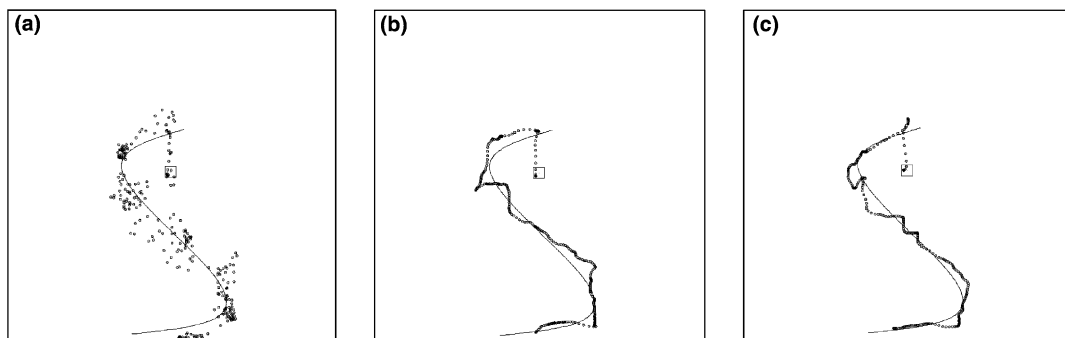


Fig. 2. Three raw traces for schemes Q0 (a), Q1 (b), and Q2 (c) (subject ML; stimulus 334). The target’s motion is indicated by the solid line. The traces shown are sampled at 25 Hz. The initial location of the target (prior to step) is indicated by the square. Pursuit for scheme Q0 was markedly different to that of Q1 and Q2, requiring rapid, wide-ranging movement of phosphene array, which may be considered nystagmus-like movements. Pursuit was more accurate for schemes Q1 and Q2; analysis across the cohort (as discussed below) shows that scheme Q2 made for better fixation and pursuit.

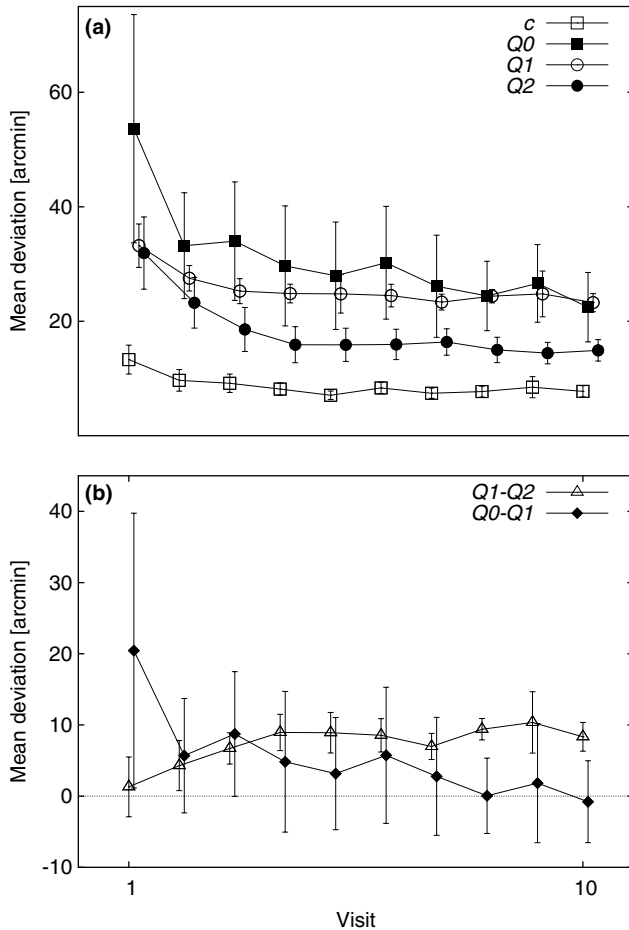


Fig. 3. (a) Subjects' mean deviation from the stationary target during fixation (in minutes of visual arc) for the three filtering schemes (Q0, Q1, Q2), and for control (c), over 10 visits. Each data point represents, for a given scheme, the cohort's average deviation from the target over the course of approximately 1.5 min fixation. The decreasing curves indicate that, with practice, subjects' fixation accuracy improved (mean deviation was reduced). (b) The relative efficacy of filtering schemes for fixation; after the first three visits, fixation is more accurate with scheme Q2 than scheme Q1; the efficacy of Q0 and Q1 is comparable (95% confidence intervals shown).

15.9 arcmin). The relative efficacy of Q2 is depicted in Fig. 3(b), as is the equivalence of Q0 and Q1.

The chief assumption for ANOVA to hold is that variance from data group to data group is approximately equal. Contrarily, the variance of mean deviation of fixation,  $\overline{f_{sfb}}$ , for both schemes Q1 and Q2, decreased with successive visits. As discussed in Snedecor and Cochran (1980, pp. 287–288), where the relationship of the variance to the mean can be determined, say,  $s^2 = \phi(\overline{f_{sfb}})$ , a transformation exists, involving the indefinite integral of the relationship, that renders the variance independent of the mean. Thus ANOVA may be performed in keeping with the chief assumption. Therefore, for each visit, the Q1 and Q2 data were pooled and the mean and variance calculated. A linear regression was then performed in  $(\overline{f_{sfb}}, s^2)$  so as to determine  $\phi(\overline{f_{sfb}})$ .

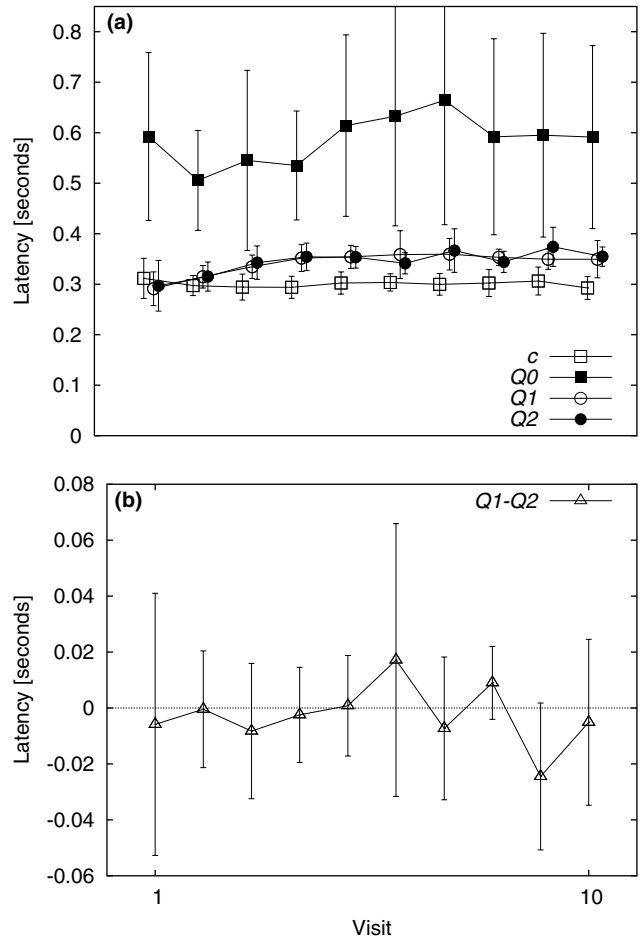


Fig. 4. (a) Latency of response to the commencement of target motion. Each data point represents the average latency of 20 saccades by each of 10 subjects. (b) The contrast between latency for Q1 and Q2 demonstrates no discernable effect of scheme Q2 as compared with Q1 (95% confidence intervals shown).

Ultimately, we derived the following variance-stabilizing transformation:  $0.310\sqrt{-55.906 + 6.444\{\cdot\}}$ .

ANOVA of the pooled Q1, Q2 fixation data revealed a strong *subject* effect ( $F(19,171) = 11.05$ ;  $P < 0.0001$ ), indicating that subjects who performed well on a given task tended to perform well elsewhere. In quantifying the efficacy of Q2 relative to Q1, the *filter*  $\times$  *visit* interaction was highly significant ( $F(9,127) = 6.97$ ;  $P < 0.0001$ ).

Fig. 4(a) depicts saccade latency for all schemes and control. Saccade data (latency and end-point) for a test were excluded according to the following criterion: if measured latency was less than 0.1 seconds, and the sensor array was therefore in motion at the time of the target's step, data were excluded. On average, latency for scheme Q0 was markedly higher than that of Q1 and Q2, which were, in turn, higher than that of control. At the conclusion of visit 10, latencies (in seconds) for control, Q0, Q1, and Q2 were 0.29, 0.59, 0.35, and 0.35, respectively. Fig. 4(b) demonstrates the

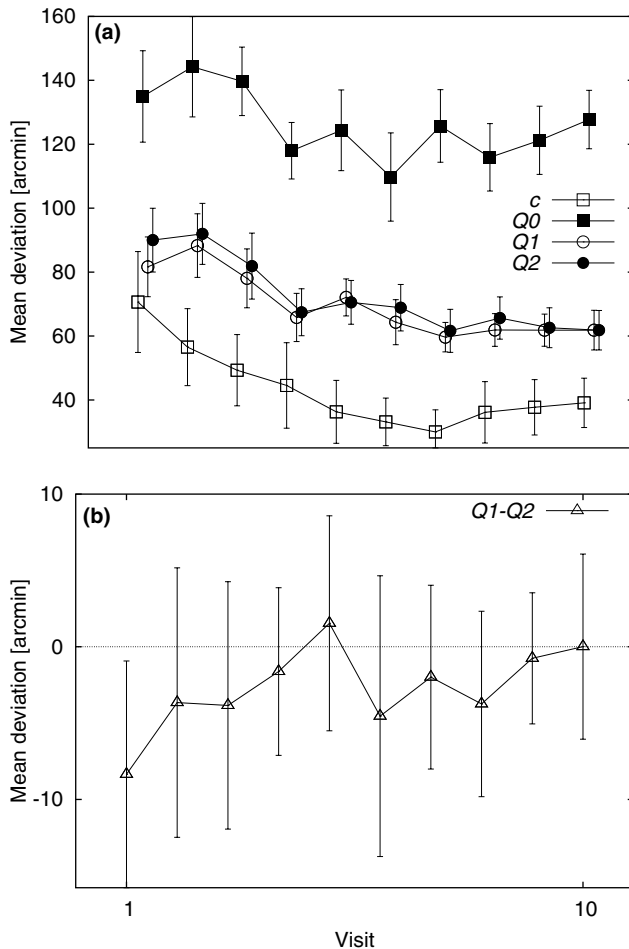


Fig. 5. (a) The mean deviation of the saccade end-point from the target for all schemes, and for control. Schemes Q1 and Q2 made for approximately equal saccade accuracy; Q0 was markedly less accurate. Again, this accuracy took practice: the bulk of learning for Q1 and Q2 occurred over the course of four visits. The contrast between schemes Q1 and Q2 (b), demonstrates their equivalency (95% confidence intervals shown).

equivalence of schemes Q1 and Q2 for latency; after repeated-measures correction, ANOVA of the pooled Q1, Q2 data yielded a *visit*  $\times$  *filter* interaction of  $F(9,170) = 0.66$  ( $P = 0.74$ ).

Fig. 5(a) depicts the learning effect on saccade end-point; with practice, subjects were better able to saccade to the target at the commencement of its motion, as measured by the deviation of the saccade end-point from the target. As for fixation and pursuit (see below), the bulk of learning of schemes Q1 and Q2 occurred within four visits. Learning was slightly protracted, however, for control (approximately six as opposed to four visits). The accuracy for schemes Q1 and Q2 was markedly better than that of Q0 (Q0, Q1, Q2 visit 10: 128.8, 67.1, 68.2 arcmin, respectively). Relative accuracy remained unchanged throughout the experiment: with practice no scheme became substantially more or less

Table 1

Median target loss per subject (first quartile, third quartile) during pursuit

	Visit 1	Visit 10
Control	0 (0.0,0.0)	0 (0.0,0.0)
Q0	16 (11.3,20.8)	12 (8.0,20.0)
Q1	0 (0.0,0.8)	0 (0.0,0.0)
Q2	0 (0.0,1.0)	0 (0.0,0.0)

Target loss (as defined in Section 2) was negligible for schemes Q1 and Q2, and for control. After approximately 50 min practice with scheme Q0 (at the conclusion of visit 10), median target loss had declined from 16 to 12.

effective than another. The contrast between schemes Q1 and Q2 is depicted in Fig. 5(b): there is little evidence to suggest that either made for better saccade end-point accuracy. Indeed, ANOVA on the pooled Q1, Q2 data exhibited the equivalence of the two schemes: the *filter*  $\times$  *visit* interaction:  $F(9,170) = 0.67$  ( $P = 0.74$ ).

Table 1 depicts target loss for all subjects for visits 1 and 10. Target loss was negligible for control, Q1, and Q2; we posit that the losses that did occur were as likely due to unfamiliarity with the task as they were visually mediated. Target loss for scheme Q0 is of interest: a median of 16 losses per subject for visit one declined to 12 for visit 10. Analysis shows that this decline falls short of significance ( $t_{19} = 1.65$ ;  $P = 0.1$ ). We would attribute this marginal result, in the main, to the fact that the cohort learned to increase sensor array movement over the course of the experiment (this is discussed further in light of Fig. 7).

Throughout the experiment, schemes Q1 and Q2 were markedly better for pursuit as compared with Q0. A practice effect was present for all schemes (and for control), as depicted by the decreasing curves of Fig. 6(a). The bulk of learning occurred over the course of four visits for schemes Q1 and Q2, and six visits for Q0. At the conclusion of visit 10, average pursuit deviations for control, Q0, Q1, and Q2 were 19.5, 124.9, 48.2, and 44.9 arcmin, respectively.

Fig. 6(b) depicts the contrast between schemes Q1 and Q2. Without practice (at the conclusion of visit one), scheme Q1 was more effective for pursuit than Q2. With four visits' practice (approximately 20 min practice with each scheme), however, the relative efficacy of Q2 was pronounced (an improved accuracy of 3.3 arcmin); this relative efficacy persisted for visits five through 10.

For purposes of ANOVA, and by the rationale and methods described above, Q1 and Q2 pursuit scores were pooled and transformed via  $0.479\sqrt{-111.938 + 4.179\{\cdot\}}$ . The pursuit data, like the fixation data, exhibited a strong *subject* effect ( $P < 0.001$ ). In assessing the Q1–Q2 contrast, the *filter*  $\times$  *visit* interaction is strongly statistically significant:  $F(9,158) = 14.23$  ( $P < 0.0001$ ).

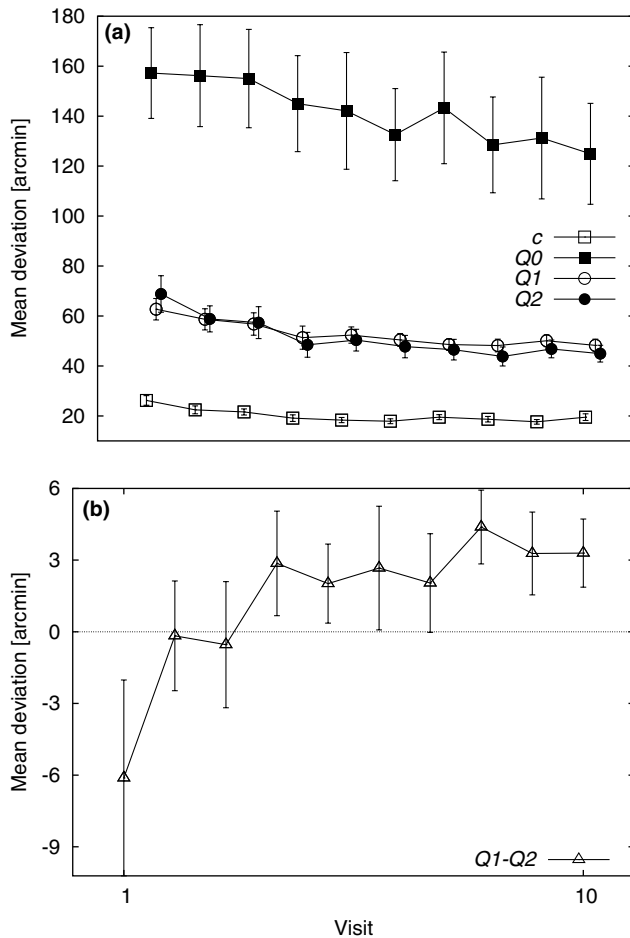


Fig. 6. (a) Subjects' mean deviation during pursuit from the target (in minutes of visual arc) for the three filtering schemes, and for control, over 10 visits. Each data point represents the cohort's mean deviation from the target over the course of approximately 5 min tracking by each of 20 subjects; the decreasing curves are indicative of the practice effect. (b) The contrast, Q1–Q2, demonstrating the relative efficacy, with practice, of scheme Q2. The improvement for scheme Q2 outstrips that of Q1 with statistical significance, as discussed in the text (95% confidence intervals shown).

### 3.2. Sensor array movement during pursuit

Power spectra of the pursuit deviation signals for visits 1 and 10,  $p_{sfl,1,10}$ , for schemes Q0–Q2 and control are depicted in Fig. 7. For all power spectra, the 99.9%-bandwidth (the frequency band containing 99.9% of signal energy), was contained in 0–5 Hz, an observation consistent with results from other human movement studies involving similar manipulanda (Ghous & Neilson, 2002). Accordingly, figures are confined to this band.

RMS velocities and accelerations for all schemes, and control, at visit 10 are contained in Table 2. Paired comparison shows that scheme Q2, as compared with Q1, required less acceleration in both the  $x$ - and  $y$ -directions. Comparison of velocities, however, is less conclusive:

the  $x$ -direction velocity for Q2 is less than that of Q1; the  $y$ -direction velocities were equal.

## 4. Discussion

Subjects were afforded simulated prosthetic vision, that is, an array of phosphenes that could be moved around the computer monitor using a joystick. Capable prosthetic visual fixation, saccade, and smooth pursuit were demonstrated in response to a small, high-contrast target. In previous studies, the *intensities* of the (fixed-size) phosphenes comprising the array were modulated according to the “underlying” stimulus (Cha et al., 1992a, 1992b; Cha, Horch, Normann et al., 1992; Humayun, 2001; Hayes et al., 2003; Thompson et al., 2003). In the present set-up, however, the *sizes* of the (fixed-intensity) phosphenes were modulated. Since the field of retinal prosthesis is relatively new and there are few *in vivo* data, it remains conjectural as to whether a device will ultimately effect the repeatable modulation of phosphene sizes or intensities; bidomain modeling of extracellular stimulation of slabs of neural tissue indicates that it may indeed be both (Roth & Wiksw, 1984). In the literature, however, it is the modulation of phosphene intensities that has received all of the attention. Our data suggest that the modulation of phosphene size will likewise produce good psychophysical results.

In driving the phosphene array, three different image analysis schemes were tested: impulsive sampling (Q0), regional averaging (Q1), and overlapping Gaussian filtering (Q2). The former two are trivial in the signal processing sense, and form the basis of previous studies; Q2 was an ad hoc design by the present authors. Our data show that Q2 afforded subjects improved fixation and pursuit accuracy as compared with both Q0 and Q1. The effective use of Q2, however, required practice; initially, Q2 was being used less effectively than Q1, but after four visits it was being used more effectively. Schemes Q1 and Q2 enabled more accurate saccades as compared with Q0, but no systematic difference between the two—Q1 and Q2—was observed.

As per Figs. 4 and 5, increased saccade accuracy was concomitant with increased latency; for schemes Q1 and Q2, latencies were an average of 60 ms longer at visit 10 as compared with visit 1 (approximately 290 ms versus 350 ms). This indicates that subjects adopted the strategy of delaying, so as to observe target motion, prior to initiating a more accurate saccade. Gellman and Carl (1991), in oculomotor studies, showed that when the motion of a target is observed prior to saccade onset, saccade accuracy is improved. In the present study, it is somewhat surprising that Q2, while having improved fixation and pursuit accuracy, did not improve saccade accuracy. This suggests that, for the extra information

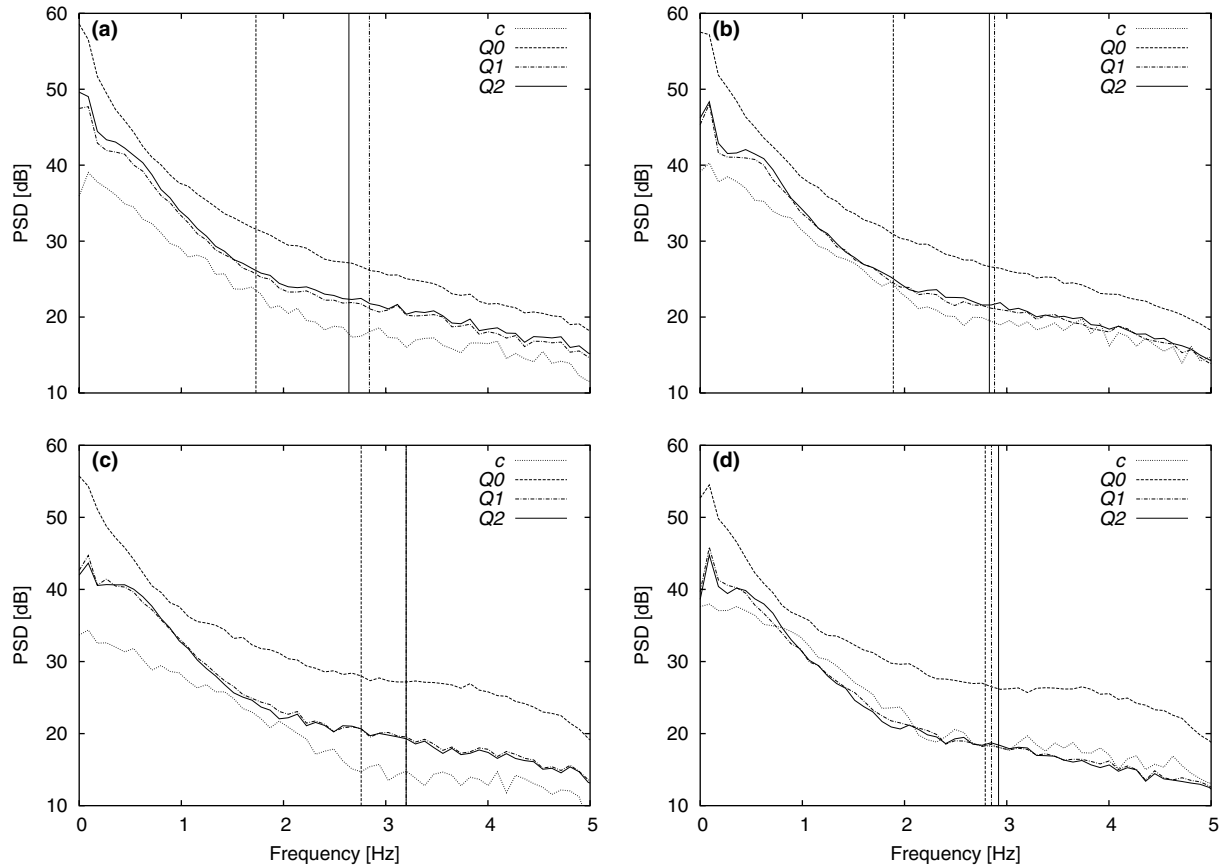


Fig. 7. (a) Power spectra of pursuit deviation signal in the *x*-direction for all schemes and control at visit 1. The PSD for scheme Q0 is greater at all frequencies from 0 to 5 Hz, indicating the extra energy required to use the scheme effectively. Vertical lines indicate 99%-bandwidths for Q0, Q1, and Q2. (b) As per (a) for *y*-direction. (c) As per (a) at visit 10. Note the marked shift in 99% bandwidth for scheme Q0 (1.73 Hz at visit 1 to 2.76 Hz), reflecting the fact that subjects learned to move the sensor array very rapidly in order to better track the target. (d) As per (c) for *y*-direction.

Table 2

Root-mean-square velocities and accelerations, in the *x*- and *y*-directions, of pursuit deviation signal,  $p_{s/10}$  (visit 10), for the three schemes and control

	Velocity [ $\text{arcmin s}^{-1}$ ]		Acceleration [ $\text{arcmin s}^{-2}$ ]	
	<i>x</i> -dir	<i>y</i> -dir	<i>x</i> -dir	<i>y</i> -dir
Control	1.99	3.01	0.79	1.17
Q0	7.21	6.51	2.61	2.32
Q1	3.23	2.72	1.16	0.97
Q2	3.18	2.72	1.12	0.93

$t_{19} = 1.78$  (Q0 vs Q1),  $t_{19} = -0.12$  (Q1 vs Q2),  $t_{19} = 2.88$  (Q0 vs Q2),  $t_{19} = 1.97$  (Q1 vs Q2),  $P = 0.09$ ,  $P = 0.91$ ,  $P = 0.01$ ,  $P = 0.06$

Two-tailed, paired (by subject) *t*-tests were employed in assessing the contrast Q1–Q2, with results indicated by braces. Less acceleration was inherent to the movement of the sensor array for scheme Q2 as compared with Q1. As per Section 4, less phosphene array velocity and acceleration are desirable features of a scheme.

encoded by scheme Q2 to be of benefit over Q1, more than 60 ms is needed by an observer to effectively temporally integrate the phosphene array. It is interesting to think of scheme Q0 as posing a sampling deficit—a deficit which would have made it impossible to observe the motion of the target prior to initiating a saccade. It is therefore not surprising that subjects adopted no such strategy for Q0. In the amblyopic eye, where there exists a spatial visual deficit, an increased saccade latency of 60 ms has been demonstrated (Ciuffreda, Kenyon, & Stark, 1978). In the normal eye, a typical saccade latency

is approximately 200 ms. Mackensen (1958) measured a 100 ms increase in hand–eye reaction time in amblyopes. In the present study, saccade latency for Q0 was approximately 300 ms slower than those of Q1 and Q2.

With practice, subjects tracked the target with better accuracy (for fixation, saccade, and pursuit). The bulk of learning had occurred by the end of the fourth visit, that is, after approximately 10 min tracking on four different days with each analysis scheme. Gauthier and colleagues (Gauthier, Vercher, Ivaldi, & Marchetti, 1988) observed time-courses similar to these for learning in

ocular and oculomanual tracking: children’s improvement was marked over the course of 4–5 one-hour trials, while adults took “several [but fewer] trials”. Karni and Sagi (1993) examined pre-attentive texture discrimination and proposed that neuronal plasticity in the cortex is central to the latent phase learning they observed: subjects’ visual sensitivity was markedly better 22–28 h after the conclusions of sessions spaced 1–3 days apart, but within-session improvement was minimal. In the present study, successive visits were separated by an average of 3.4 days (s.d. 2.5). It is interesting to note that Karni and Sagi observed, as did we, decreased variance (increased consistency) concomitant with increased performance (in the present case, decreased deviation).

To quantify the time-courses of learning, we fitted the following exponential to the fixation and pursuit mean deviation data:

$$a \times \exp\left(\frac{-\text{visit}}{b}\right) + c. \quad (2)$$

The curves are depicted in Fig. 8. Least-squares fitting was performed using R (2004), a language and environment for statistical computing, which implements the Gauss–Newton algorithm. Of particular interest is the parameter  $b$ , which may be thought of as a learning time-constant. That is, analogous to the time constant of an RC electric circuit which describes the time-course of voltage decay, it denotes the period during which approximately 67% of learning occurs. For fixation, the time-constants for Q1 and Q2 were 1.0 and 1.3, respectively. For pursuit, the time-constants for Q1 and Q2 were 2.9 and 2.3, respectively.

In addition to improved accuracy, our data suggest that appropriate image processing would make for less requisite movement of the phosphene array; pursuit via scheme Q2, as compared with Q1, required slightly less (albeit statistically significant) velocity and acceleration. Reduced requisite movement would likely be of clinical benefit. Early generation prostheses will likely involve a head-mounted camera (Suaning, Hallum, Chen, Preston, & Lovell, 2003); in subsequent generations the camera may be contained wholly within the eye (Hamill, Kuppermann, Fine, & Lane, 2003). The former would require head movements, and the latter modified eye movements (modified due to the introduction and affixment of implantable components to the ocular anatomy), to replace, as best as possible, eye movements integral to normal vision. Therefore, for a prosthesis, increased velocities and accelerations refer to those of the head or eye. If we consider the case of a head-mounted camera, a scheme requiring more accelerations may make for adverse vestibular reactions like those observed by Cha et al. (1992a) in mobility studies. Further, Schieppati, Nardone, and Schmid (2003) demonstrated that balance is adversely affected via afferent inflow after induced neck muscle fatigue in standing

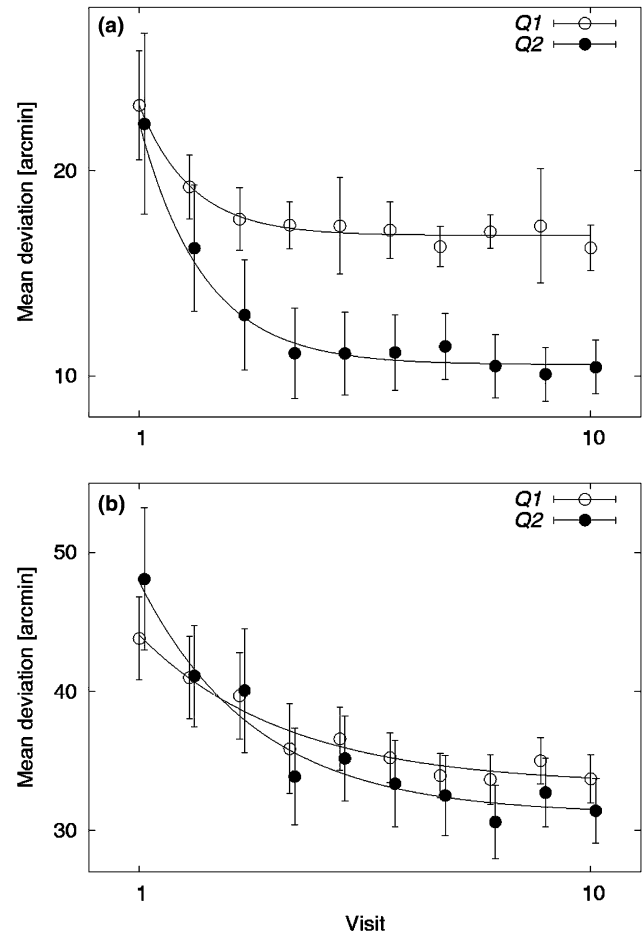


Fig. 8. Fixation (a) and pursuit (b) data with exponentials fitted for schemes Q1 and Q2. Learning for fixation occurred more quickly than for pursuit. The intersecting curves in (b) show that the relative effective use of Q2 required practice. Residual sum-of-squares, (a) Q1 and Q2: 1.1 and 1.4, respectively; (b) Q1 and Q2: 4.9 and 11.9, respectively.

subjects, a result that was exacerbated when subjects were deprived of visual input. The Schieppati result may have played a role in the aforementioned dizziness observed by Cha et al. (1992a). In Appendix A, we have demonstrated briefly, via simple mechanics, how increased acceleration and velocity contribute to muscle fatigue. Muller, Stoll, and Schmal (2003) measured reduced peak velocities in eyes of contact lens-wearing subjects as compared with controls wearing glasses. Those authors hypothesized that the additional mass of the contact lens may be a contributing factor. The introduction of an implantable electronic prosthetic device to the ocular anatomy will, too, alter the eye’s normal mechanics. Usually, the eye’s centre of mass and centre of rotation approximately coincide (Maddox, 1907, pp. 68–78), minimizing the system’s moment of inertia—its resistance to rotation. An implanted device, however, introduces an inertial mass to the system. So, for a wholly intraocular device, movement may be

restricted to lesser velocities and accelerations. Thus, an image processing scheme that enables accurate pursuit at lesser velocities and accelerations may be of benefit.

In the present tracking task, further to its affording better accuracy, Q2 is characterized by slightly smaller velocities and accelerations than the other schemes. Our data are indicative of, although not equivalent to, those we would expect from a patient with a head-mounted or wholly intraocular prosthesis. The extent to which they are indicative lies in the extent to which movement of the hand in oculomanual tracking (eye-and-hand; EH) is analogous to movement of the eye in ocular tracking (eye alone; EA) and to head movement. Xia and Barnes (1999) compared EA and EH tracking and demonstrated the equivalent accuracy of the hand (in EH tracking) and the eye (in EA tracking) for target frequencies up to approximately 2 Hz. In response to increased target velocity, both hand and eye responses broke down. Hand break-down was faster than that of eye, but this occurred at target velocities upwards of 18 deg/s, markedly higher than those used in the present experiment (approximately 2 deg/s). Jacobs and van Steenberghe (1993) compared finger tracking and head tracking (in response to target velocities no greater, we estimate, than 1.2 deg/s). They reported both finger and head signals that generally lagged the target signal (approximately 0.25 s and 0.5 s lag, respectively) and exhibited low-frequency oscillations about the target. Cross-correlation and spectral analysis revealed no significant difference, however.<sup>2</sup> Gauthier et al. (1988), in EA and EH studies, reported a smooth pursuit saturation velocity of 40 deg/s for the eye and a pursuit saturation velocity of 90 deg/s for the hand. Taken together, these studies indicate that it is reasonable to expect accurate tracking by hand as by eye and head for targets at velocities like those we have used, despite the fact that eye and hand movements are different dynamically. Eye movements are comprised of slow and fast phases (smooth pursuit and saccade, respectively) (Leigh & Zee, 1999, pp. 90–186), whereas hand movement is more continuously graded (a concise demonstration of this involves ocular tracking of a self-moved target, wherein the frequency response of the oculomotor system is effectively “pulled up” by the presence of the hand (Vercher, Volle, & Gauthier, 1993)). Of important note is the trade-off between the phases of eye movement (as numerous studies demonstrate, e.g. Vercher et al. (1993)): in the case of deteriorating smooth pursuit, an increase in saccadic eye movements serve to keep the target better foveated (this is the case be it induced by a

changed, say, faster, stimulus (e.g. Vercher et al. (1993)), or the result of disease, such as the abnormal saccadic substitution observed in amblyopic eyes (Ciuffreda, Kenyon, & Stark, 1979)). Further, since the “main sequence” relationship dictates that a saccade of greater amplitude will attain higher peak velocities (Boghen, Troost, Daroff, Dell’Osso, & Birkett, 1974), it follows that, as smooth pursuit accuracy deteriorates increasingly, saccade velocities increase. What we have demonstrated in the present study is an analysis scheme (Q2) that enables better accuracy. It follows that, when integrated with a prosthetic visual system, the scheme would require of patients fewer saccades or correcting movements. It is these corrections that involve greater velocities and accelerations.

Since a more dense packing of more phosphenes makes for better prosthetic vision, the question arises, Why not simply pack more phosphenes more densely? In vitro physiological studies have demonstrated the efficacy of electrodes separated by 25  $\mu\text{m}$  (corresponding to 5.1 min of visual arc) in activating retinal neural tissue (Grumet, 1999); this work casts promising light on the possible restoration of high-resolution, or normal, vision. In vivo trials in human sufferers of retinal degeneration, however, have shown that small electrodes are in fact unreliable in rendering phosphenes (Rizzo, Jensen, Loewenstein, & Wyatt, 2003). Greenberg has suggested that, for the electrode configuration he used, electrode separation distance is likely to be no less than 0.25 mm (0.8°), the distance at which a 3 dB rise in stimulation threshold is observed in the frog (Greenberg, 1998); Humayun et al. (1999) reported that blind human patients could discern 435  $\mu\text{m}$  (1.5°) electrode separation distances. A recent clinical trial involves electrodes with centre-to-centre spacing of 720  $\mu\text{m}$  (2.4°) (Humayun et al., 2003b). For comparison’s sake, again, we turn to multi-channel cochlear neuroprostheses: animal studies indicate that bipolar stimulation results in more restricted fields of excitation (Kral, Hartmann, Mortazavi, & Klinke, 1998) (indeed, it was widely held for years after the advent of the implant that only bipolar stimulation could activate discrete regions of spiral ganglion cells (Rubinstein & Miller, 1999)), but, psychophysically, bipolar and monopolar stimulation have proven equivalent for speech recognition (Zwolan, Kileny, Ashbaugh, & Telian, 1996). Intraocular electrode arrays with dimensions of the order of tens of micrometers may be decades in the realization; the realization of an implantable device will precede a full understanding of the electrode–tissue interface in situ. Further, thousands of small electrodes would pose higher power demands on implanted integrated circuitry, since resistivity is inversely proportional to cross-sectional area. The two foremost application-specific integrated circuits (Suaning & Lovell, 2001; Liu et al., 2000), propose the transmission of data and power via radio frequency;

<sup>2</sup> Of note is the fact that Jacobs and van Steenberghe observed similar head and finger responses to delayed visual feedback. They posit that this similarity is as expected, since visual feedback is naturally integral to both finger and head movement.

furthermore, a portable prosthesis would be powered by battery, for which increased power dissipation means accelerated discharge time.

With regard to densely packing phosphenes, in this experiment we arrayed phosphenes in a regular hexagonal mosaic; all previous approaches have arrayed phosphenes in a regular rectangular layout. The overall dimensions of the visual simulations employed in the present work make for activation of a region of the retina that approximately corresponds to proposed electrode array geometries (Suanning et al., 2003). Our hexagonal approach is based on the reasonable assumption that an electrode activates adjacent retinal neural tissue, and that the activated region is approximately circular. Rizzo et al. (2003) have shown, in stimulating the excised retina with small, spherical, extracellular electrodes, that there exists some ganglion cell activation at small distances beyond the diameter of the electrode. Thus, the problem as to how to densely pack phosphenes in the visual field becomes a question of geometry. It is widely known that the densest packing of equisized circles on an unbounded plane is a regular hexagonal mosaic. This result was proven by Fejes Tóth in 1940. Accordingly, it may be efficacious to manufacture hexagonal arrays of implantable electrodes. At minimum, we posit that said manufacture should take into account phosphene geometry, and geometric packing results. We have discussed dense phosphene packing, and its advantages, more quantitatively in previous work (Hallum, Suanning, & Lovell, 2004).

## 5. Conclusion

Our data demonstrate a small though significant improvement in simulated prosthetic visuo-motor function for an image analysis scheme involving overlapping Gaussian kernels. In the information theoretic sense, the scheme better encodes the stimulus within the confines of prosthetic vision (the synthesis parameters). This is the first step of an experimental, heuristic process; the phosphene array movement data accrued here should allow revised, more effective image analysis designs with a mind to further improving fixation, saccade, and pursuit, and addressing more complex visual tasks such as visual search. The present approach and its development will likely improve clinical outcomes of retinal prosthetic devices.

## Acknowledgment

The authors would like to thank Phil Preston for joystick design and discussions, Ross Odell for discussions regarding the statistics, and John Morley for discussions regarding the psychophysics.

## Appendix A

The energy generated by muscle contraction is spent by way of mechanical work and heat (for a concise treatment, see Epstein & Herzog, 1998, pp. 16–18). Therefore, in assessing the vigor of phosphene array movement, we first consider power,

$$P = \mathbf{F} \cdot \mathbf{v}. \quad (3)$$

Thus, in each of the  $x$ - and  $y$ -directions, power is proportional to the product of acceleration and velocity

$$P \propto a \cdot v. \quad (4)$$

For periodic motions, the issue may be complicated by the tendency of elastic tendons and muscle to store energy (Alexander & Bennet-Clark, 1977). In such cases, the system approximates an oscillatory one wherein energy is lost due to friction alone. For example, consider the damped oscillations of a pendulum that comes to rest over time. The common, simple model for friction states that frictional (drag) force is proportional to, and in the opposite direction of, velocity (for concise discussion, see Tipler, 1991, p. 388):

$$\mathbf{F}_d = -b\mathbf{v}, \quad (5)$$

where  $b$  is a damping constant, and  $\mathbf{v}$  is the velocity of motion. Thus, by combining Equations (2) and (4), we see that, in each direction, the power employed opposing friction is proportional to the square of velocity:

$$P \propto v^2. \quad (6)$$

It is unclear to the authors at this time the extent to which muscle and tendon elasticity will affect vigor; we mention the phenomenon here due to the highly oscillatory nature of the pursuit deviation signal. Morgan, Proske, and Warren (1978) estimated that such storage saved the hopping kangaroo 30% energy; this, however, is chiefly due to a long, compliant Achilles tendon. Alexander and Bennet-Clark (1977) addressed the problem with regard to the flight muscles of the locust. However, for insects the high frequency of wing beat renders the work done at each muscular contraction less, and therefore the relative effect of stored energy greater.

## References

- Alexander, R. Mc. N., & Bennet-Clark, H. C. (1977). Storage of elastic strain energy in muscle and other tissues. *Nature*, 265, 114–117.
- Arbogast, T. L., Mason, C. R., & Kidd, G., Jr., (2002). The effect of spatial separation on informational and energetic masking of speech. *Journal of the Acoustical Society of America*, 112, 2086–2098.
- Boghen, D., Troost, B. T., Daroff, R. B., Dell'Osso, L. F., & Birkett, J. E. (1974). Velocity characteristics of normal human saccades. *Investigative Ophthalmology and Visual Science*, 13, 619–623.

- Cha, K., Horch, K. W., & Normann, R. A. (1992a). Mobility performance with a pixelized vision system. *Vision Research*, *32*, 1367–1372.
- Cha, K., Horch, K. W., & Normann, R. A. (1992b). Simulation of a phosphene-based visual field: Visual acuity in a pixelized vision system. *Annals of Biomedical Engineering*, *20*, 439–449.
- Cha, K., Horch, K. W., Normann, R. A., & Boman, D. K. (1992). Reading speed with a pixelized vision system. *Journal of the Optical Society of America*, *9*, 673–677.
- Ciuffreda, K. J., Kenyon, R. V., & Stark, L. (1978). Increased saccadic latencies in amblyopic eyes. *Investigative Ophthalmology and Visual Science*, *17*, 697–702.
- Ciuffreda, K. J., Kenyon, R. V., & Stark, L. (1979). Abnormal saccadic substitution during small-amplitude pursuit tracking in amblyopic eyes. *Investigative Ophthalmology and Visual Science*, *18*, 506–516.
- Dorman, M. F., Loizou, P. C., & Fitzke, J. (1998). The identification of speech in noise by cochlear implant patients and normal-hearing listeners using 6-channel signal processors. *Ear and Hearing*, *19*, 481–484.
- Epstein, M., & Herzog, W. (1998). *Theoretical models of skeletal muscle*. Chichester: John Wiley and Sons Ltd.
- Eysel, U. T., Walter, P., Gekeler, F., Schwahn, H., Zrenner, E., Sachs, H. G., et al. (2002). Optical imaging reveals 2-dimensional patterns of cortical activation after local retinal stimulation with sub- and epiretinal visual prostheses. *Investigative Ophthalmology and Visual Science*, *43* (ARVO Abstract 4486).
- Fejes Tóth, L. (1940). Über einen geometrischen satz. *Mathematische Zeitschrift*, *46*, 79–83.
- Frigo, M., & Johnson, S. G. (1998). FFTW: An adaptive software architecture for the FFT. In *Proceedings IEEE International Conference Acoustics Speech and Signal Processing* (Vol. 3, pp. 1381–1384).
- Gauthier, G. M., Vercher, J.-L., Ivaldi, F., & Marchetti, E. (1988). Mussa Oculo-manual tracking of visual targets: Control learning, coordination control and coordination model. *Experimental Brain Research*, *73*, 127–137.
- Gellman, R. S., & Carl, J. R. (1991). Motion processing for saccadic eye movements in humans. *Experimental Brain Research*, *84*, 660–667.
- Ghous, A., & Neilson, P. D. (2002). Evidence for internal representation of a static nonlinearity in a visual tracking task. *Human Movement Science*, *21*, 847–879.
- Greenberg, R. J. (1998). Analysis of electrical stimulation of the vertebrate retina: Work towards a retinal prosthesis. PhD thesis, Johns Hopkins University.
- Grumet, A. E. (1999). Electrical stimulation parameters for an epiretinal prosthesis. PhD thesis, Massachusetts Institute of Technology.
- Hallum, L. E., Suaning, G. J., & Lovell, N. H. (2004). Contribution to the theory of prosthetic vision. *ASAIO Journal*, *50*, 392–396.
- Hamill, M. B., Kuppermann, B. D., Fine, I. H., & Lane, S. S. (2003). The Implantable Miniature Telescope: 12-month results of the US IMT-001 clinical trial in patients with stable age-related macular degeneration. *Investigative Ophthalmology and Visual Science*, *44* (ARVO Abstract 4209).
- Hayes, J. S., Yin, V. T., Piyathaisere, D., Weiland, J. D., Humayn, M. S., & Dagnelie, G. (2003). Visually guided performance of simple tasks using simulated prosthetic vision. *Artificial Organs*, *27*, 1016–1028.
- Hornig, R., & Eckmiller, R. (2002). Retina implant stimulator with on-chip memory for complex stimulus profiles. *Investigative Ophthalmology and Visual Science*, *43* (ARVO Abstract 4489).
- Humayun, M. S. (2001). Intraocular retinal prosthesis. *Transactions of American Ophthalmology Society*, *99*, 271–300.
- Humayun, M. S., de Juan, E., Dagnelie, G., Greenberg, R. J., Propst, R. H., & Phillips, D. H. (1996). Visual perception elicited by electrical stimulation of retina in blind humans. *Archives of Ophthalmology*, *114*, 40–46.
- Humayun, M. S., de Juan, E., Jr., Weiland, J. D., Dagnelie, G., Katona, S., Greenberg, R. J., et al. (1999). Pattern electrical stimulation of the human retina. *Vision Research*, *39*, 2569–2576.
- Humayun, M. S., Greenberg, R. J., Mech, B. V., Yanai, D., Mahadevappa, M., van Boemel, G., et al. (2003a). Chronically implanted intraocular retinal prosthesis in two blind subjects. *Investigative Ophthalmology and Visual Science*, *44* (ARVO Abstract 4206).
- Humayun, M., Propst, R., de Juan, E., Jr., McCormick, K., & Hickingbotham, D. (1994). Bipolar surface electrical stimulation of the vertebrate retina. *Archives of Ophthalmology*, *112*, 110–116.
- Humayun, M. S., Weiland, J. D., Fujii, G. Y., Greenberg, R., Williamson, R., Little, J., et al. (2003b). Visual perception in a blind subject with a chronic microelectronic retinal prosthesis. *Vision Research*, *43*, 2573–2581.
- Jacobs, R., & van Steenberghe, D. (1993). Jaw, head and finger tracking behaviour with delayed visual feedback. *Journal of Electromyography and Kinesiology*, *3*, 103–111.
- Karni, A., & Sagi, D. (1993). The time course of learning a visual skill. *Nature*, *365*, 250–252.
- Kral, A., Hartmann, R., Mortazavi, D., & Klinke, R. (1998). Spatial resolution of cochlear implants: The electrical field and excitation of auditory afferents. *Hearing Research*, *121*, 11–28.
- Leigh, R. J., & Zee, D. S. (1999). *The neurology of eye movements* (Third ed.). New York: Oxford University Press.
- Liu, W., Vichienchom, K., Clements, M., DeMarco, S. C., Hughes, C., McGucken, E., et al. (2000). A neuro-stimulus chip with telemetry unit for retinal prosthetic device. *IEEE Journal of Solid-State Circuits*, *35*, 1487–1497.
- Maddox, E. E. (1907). *Tests and studies of the ocular muscles*. Philadelphia: The Keystone Publishing Co.
- Matlab version 5.3, release 11 (1999). MathWorks Inc., Massachusetts, USA.
- Mackensen, G. (1958). Reaktionszeitmessungen bei amblyopie. *Graefes Archives of Ophthalmology*, *159*, 636.
- Morgan, D. L., Proske, U., & Warren, D. (1978). Measurement of muscle stiffness and the mechanism of elastic storage of energy in hopping kangaroos. *Journal of Physiology*, *282*, 253–261.
- Muller, C., Stoll, W., & Schmal, F. (2003). The effect of optical devices and repeated trials on the velocity of saccadic eye movements. *Acta Oto-laryngologica*, *123*, 471–476.
- R Development Core Team (2004). R: A language and environment for statistical computing. R Foundation for Statistical Computing, Vienna, Austria. ISBN 3-900051-00-3, URL: <http://www.R-project.org>.
- Rashbass, C. (1961). The relationship between saccadic and smooth tracking eye movements. *Journal of Physiology*, *159*, 326–338.
- Rizzo, J. F., Jensen, R. J., Loewenstein, J., & Wyatt, J. (2003). Unexpectedly small percepts evoked by epi-retinal electrical stimulation in blind humans. *Investigative Ophthalmology and Visual Science*, *44* (ARVO Abstract 4207).
- Roth, B. J., & Wikswo, J. P. Jr., (1984). Electrical stimulation of cardiac tissue: A bidomain model with active membrane properties. *IEEE Transactions on Biomedical Engineering*, *41*, 232–240.
- Rubinstein, J. T., & Miller, C. A. (1999). How do cochlear prostheses work? *Current Opinion in Neurobiology*, *9*, 399–404.
- Schieppati, M., Nardone, A., & Schmid, M. (2003). Neck muscle fatigue effects postural control in man. *Neuroscience*, *121*, 277–285.
- Snedecor, G. W., & Cochran, W. G. (1980). *Statistical methods* (Seventh ed.). Ames: The Iowa State University Press.
- StataCorp. 2000. *Statistical Software: Release 6.0*. College Station, Texas: Stata Corporation.
- Stone, J. L., Barlow, W. E., Humayun, M. S., de Juan, E., Jr., & Milam, A. H. (1992). Morphometric analysis of macular photoreceptors

- and ganglion cells in retinas with retinitis pigmentosa. *Archives of Ophthalmology*, 110, 1634–1639.
- Suaning, G. J., Hallum, L. E., Chen, S. C., Preston, P. J., & Lovell, N. H. (2003). Phosphene vision: Development of a portable visual prosthesis system for the blind. In *Proceedings of the 25th Annual International Conference IEEE Engineering in Medicine and Biology Society*, 2003.
- Suaning, G. J., & Lovell, N. H. (2001). CMOS neurostimulation ASIC with 100 channels, scaleable output, and bi-directional radio-frequency telemetry. *IEEE Transactions on Biomedical Engineering*, 48, 248–260.
- Suaning, G. J., Lovell, N. H., & Kwok, C. Y. (2003). Fabrication of platinum spherical electrodes in an intra-ocular prosthesis using high-energy electrical discharge. *Sensors and Actuators A—Physical*, 108, 155–161.
- Thompson, R. W., Jr., Barnett, G. D., Humayun, M. S., & Dagnelie, G. (2003). Facial recognition using simulated prosthetic pixelized vision. *Investigative Ophthalmology and Visual Science*, 44, 5035–5042.
- Throckmorton, C. S., & Collins, L. M. (2002). The effect of channel interactions on speech recognition in cochlear implant subjects: Predictions from an acoustic model. *Journal of the Acoustical Society of America*, 112, 285–296.
- Tipler, P. A. (1991). *Physics for Scientists and Engineers* (Third ed.). New York: Worth.
- Vercher, J.-L., Volle, M., & Gauthier, G. M. (1993). Dynamic analysis of human visuo-oculo-manual coordination control in target tracking tasks. *Aviation, Space, and Environmental Medicine*, 64, 500–506.
- Xia, R., & Barnes, G. (1999). Oculomanual coordination in tracking of pseudorandom target motion stimuli. *Journal of Motor Behavior*, 31, 21–38.
- Zrenner, E. (2002). Will retinal implants restore vision? *Science*, 295, 1022–1025.
- Zwolan, T. A., Kileny, P. R., Ashbaugh, C., & Telian, S. A. (1996). Patient performance with the Cochlear Corporation '20 + 2' implant: Bipolar versus monopolar activation. *American Journal of Otology*, 17, 717–723.